Proceedings of the 7th International Young Geotechnical Engineers Conference – Scott (Ed.)

Cyclic degradation of axially loaded piles installed in micaceous silty soil

Dégradation cyclique de pieux sous charge axiale et installés dans un sol micacé et limoneux.

Guillaume Melin, Shahrooz Rezvani, Søren P.H. Sørensen & Kristine Lee Kaufmann
Wind & Renewables, COWI A/S, Denmark, gmme@cowi.com

ABSTRACT: This paper presents the learnings from the recent detailed design of an offshore wind farm in Taiwan. The foundations consist of four-legged jackets supported on pre-piled hollow-steel piles. For jacket foundations, the axial pile capacity is governing the required embedded length. Due to cyclic loading from wind and waves, an assessment of the effects of cyclic loading on the axial pile capacity is essential. The focus of this paper is the cyclic concept adopted for the detailed design. To assess the behaviour of the site-specific soil to cyclic loading, a series of cyclic direct shear constant normal stiffness tests have been performed. Most of these have been performed in stress-controlled state and a few tests in displacement-controlled state. Based on the these tests a degradation law has been determined relating the cyclic degradation to the cyclic stress ratio and the number of load cycles. This degradation law has been adopted in a 1D model of a single pile. From this 1D model a cyclic pile interaction diagram has been developed. The cyclic degradation of the axial pile capacity caused by the design storm event has been predicted using published axial capacity degradation models adopting the cyclic pile interaction diagram.

RÉSUMÉ : Cet article présente les enseignements tirés de la récente conception détaillée d'un parc éolien en mer à Taiwan. Les fondations consistent en des structures de type “jacket”, à quatre pieds, supportées par des pieux tubulaires en acier. Pour ce type de fondation, la capacité portante des pieux régit la longueur d'encastrement requise. En raison de la charge cyclique due au vent et aux vagues, une évaluation des effets de la charge cyclique sur la capacité portante des pieux est essentielle. Le présent document se concentre sur la méthode adoptée pour la conception détaillée. Pour évaluer le comportement du sol face à la charge cyclique, une série d'essais cycliques de cisaillement direct à rigidité normale constante a été réalisée. La plupart de ces essais a été réalisée avec un taux de contrainte contrôlé et quelques essais avec un taux de déformation contrôlé. En résulte une loi de dégradation reliant la dégradation cyclique au rapport de contrainte cyclique et au nombre de cycles de charge. Cette loi a été adoptée dans un modèle uni-dimensionnelle du pieu avec courbes t-z. A partir de ce modèle, un diagramme d'interaction cyclique a été développé. La dégradation cyclique de la capacité axiale du pieu est calculée en utilisant des modèles publiés de dégradation cyclique et en s’appuyant sur un diagramme spécifique aux différentes fondations du parc éolien en question.

KEYWORDS: offshore, mica, cyclic-loading, degradation, pile.

1 INTRODUCTION

1.1 *Offshore Wind in APAC region*

The offshore wind pioneers of the 90s knew what potentials harnessing the power of wind at sea would have on a global scale but even the most optimistic would perhaps struggle to see the transformative role offshore wind has played in the global energy mix.

2019 witnessed a record breaking 6.1GW of new installed capacity globally, from which Asia excluding China contributed to 2% of market share. Taiwan has planned installing an additional 15GW by 2035 which will see it becoming the second leading contributor in Asia (GWEC 2021). Unlike European sites, the Taiwanese wind farms have to be designed for extra resilience in order to withstand the impact of local environmental conditions such as currents, typhoons and earthquakes. Duty of care dictates a diligent approach integrating European design expertise with local regulatory standards without penalizing the design for encompassing harsh marine environments. This paper delves into the state-of-the-art efforts and its benefits in improving the geotechnical design approaches and predicting the behaviour of bearing capacity of the jacket foundation piles.

1.2 *Site conditions*

The site is bound, physically and metaphorically, by challenging soils, seismic activities, largest global sediment inpour from mountainous rivers and the most intensive monsoon system. The combined effect of which in load transfer requires in depth understanding of the underlying stratigraphy.

The soils, characterizing the underlying stratigraphy considered in design, are largely from the Quaternary epoch. A detailed position-specific site investigation campaign was carried out, and the findings suggested highly layered soils of sandy, silty and clayey nature. Sand and silt were found to be of loose to medium dense with traces of shell fragment and mica specks. The soils were found to be extensively silty. Clay, albeit not present extensively, was found to vary in strength, from soft to stiff.

1.3 *Jacket foundations*

Jacket substructure with pre-installed foundation piles were found to be the most feasible solution in counteracting the constraints associated with environmental conditions due to seasonal typhoon and seismic loading together with water depths of 15 m to 30 m and in the presence of normally consolidated soils.

Whilst it is common to design the substructure per cluster, the foundation piles are designed per WTG location thus being fully attuned to the position specific conditions. The piles were designed with a diameter of 3.1 m and total lengths (including 1.5 m stick up) varying from 63 m to 82 m across the site.

1.4 *Purpose of paper*

This paper delves further into project specific considerations that were applied in design regarding the loading mechanism specific to this Taiwanese offshore windfarm, as light weight turbines may induce axial cyclic degradation thus leading to tension loading becoming as dominating as compression loading.

Efforts are made to illustrate the premise between the element laboratory testing proposed and the geotechnical design of the foundation piles allowing for a more accurate approach to design. The traditional approach to design for these piles comprised API framework. In recent years, due to API shortcomings concerning the lack of reliability in sand amongst others, the offshore industry is considering CPT based methods as being representative of in-situ conditions. The rationale behind the site

investigation campaign together with associated laboratory testing and its application to design is discussed in more details further in the paper.

2 SOIL-PILE INTERACTION

2.1 *Axial pile capacity*

The design embedment length of jacket pin-piles is typically governed by the axial resistance of the piles.

State-of-the-art pile capacity methods must be envisaged to capture the proper stress state around the pile after installation and ensure an optimized design. As it is a common, and highly recommended, practice in the offshore wind industry to perform cone penetration testing (CPT) at all positions across a site, CPT-based methods to calculate the capacity of a pile may be considered, cf. Jardine et al. (2005) or Lehane et al. (2007 and 2013).

A sensitivity study carried out for the site showed that the API method (API, 2014) yielded larger capacities than the NGI (Clausen et al., 2005; Karlsrud et al., 2005), the UWA (Lehane et al., 2007 and 2013) and the ICP (Jardine et al., 2005) CPT-based methods. These CPT based methods are for most soil conditions considered to perform better than the API method, cf. Gavin et al. (2011). Moreover, CPT-based methods are sought as relying on more recognised mechanism of the behaviour of piles under axial loads, e.g. the friction fatigue concept. The use of CPT-traces, a physical measurement, as a direct input in the CPT-based methods is also considered as a strong argument in favour of CPT-based methods. Consequently, CPT-based methods were deemed appropriate for the site.

2.2 *Winkler foundation*

In offshore geotechnics, pile foundations are typically represented as a beam supported by independent springs, the so-called Winkler approach, cf. Winkler (1867). Those springs represent the load reaction curves of the soil resistance. Axial load-displacement curves were developed by API (2014), together with its well-known axial pile capacity calculation method.

Load reaction curves along the pile (t-z) were therefore normalized for the maximum load reaction t_{max} to reach the shaft resistance per given meter length of pile as per CPT-based method, and similarly for the load reaction curve at the pile tip (Q-z), normalized to the maximum tip resistance Q_{max}.

3 CYCLIC DEGRADATION

3.1 *Effect of cyclic lateral loading*

Cyclic lateral loading may lead to reductions of the axial shaft resistance. As such, loading may cause gapping and pore-pressure build-up causing a loss of the effective radial stress on the pile. Gapping effects mainly occurs for stiff to hard fine-grained materials, whilst pore-pressure build-up may occur both for fine-grained and coarse-grained materials. The effects of cyclic lateral loading on the axial pile response are concentrated in the upper part of the pile for which significant lateral pile deflections occur, whilst the axial shaft resistance of the lower part of the pile is unaffected by the cyclic lateral loading.

Argiolas and Jardine (2017), Hampson et al. (2017), and Merritt et al. (2012) have proposed simplified methods for evaluating the effect of cyclic lateral loading on the axial shaft resistance. The methods proposed by Argiolas and Jardine (2017) and Hampson et al. (2017) are developed for hard clay tills and consider the effect of a zone of gapping between soil and pile for which the axial shaft resistance is reduced to zero and an influence zone over which the shaft resistance is partially reduced. The method proposed by Merritt et al. (2012) is developed primarily for coarse-grained materials for which the cyclic lateral loading may cause pore-pressure build-up, but where only limited gapping is expected.

Given the ground conditions at the Project, which is heavily stratified consisting of mixtures of sands, silty sands, sandy silts, clayey silts and clays, the risk of gapping between soil and pile is considered negligible. Therefore, the simplified approach of Merritt et al. (2012) has been considered. This approach relies on the findings of Dührkop (2010).

3.2 *Effect of cyclic axial loading*

Cyclic degradation of pin-piles under axial loading is another complex soil-pile interaction problems for pile foundations that engineers face during foundation design. No methodologies have yet penetrated the recommended practices or standards in the offshore geotechnics community. Axial loading on the pile is sought of mobilising the full shaft resistance at 1% pile diameter of pile displacement relative to the soil (API, 2014). The end bearing however is fully-mobilised at much larger pile toe displacement. Hence, it may be simplified that axial cyclic loading on the piles primarily mobilise the upper part of the pile, or may in some larger loading conditions, affect the whole shaft resistance without particularly mobilising the end-bearing.

Considering this complex pile-soil interaction, large-scale pile load tests may be performed to mimic the cyclic loading onto the pile and its subsequent behaviour. Such pile load tests have been performed and published for a number of site conditions and pile-soil interaction diagrams have been constructed to reflect the load level and number of cycles at which failure of the pile is observed.

Diagrams such as the cyclic stability diagram by Poulos (1989) in which the abscissa and ordinates respectively represent the loading conditions for a mean and a cyclic component are found in the literature to understand the impact of axial cyclic loading on the pile stability. Poulos' diagram is divided into several zones where cyclic loading is reported to have more or less impact onto the pile capacity.

Jardine et al. (2005) and Kirsch and Richter (2011) both present similar cyclic stability diagrams specific to conducted pile tests. From a designer's perspective, such knowledge cannot directly be used due to their inherent site-specific nature. Furthermore, soil deposits in the Taiwanese strait come from large sediment transport and are likely to respond differently compared to the available published data unless proven otherwise. Eventually, the need of creating cyclic interaction diagrams from scratch for each location of interest across the site was necessary. The method described in the paper therefore relies on the site-specific laboratory campaign and site-specific loading conditions to avoid the drawbacks mentioned above.

4 LABORATORY CAMPAIGN

4.1 *Intro to site investigations*

A WTG location specific site investigation was carried out to characterise the site conditions and inform the dynamic design of foundation piles as well as the global stiffness of the system. An intrusive campaign consisting of CPTu and sampling borehole was undertaken. A bespoke testing regime was formulated accounting for boundary conditions, input and expected range of parameters, to address the complex loading mechanism and the potential cyclic degradation impacting the design.

The laboratory testing campaign was designed to verify the assumptions made as part of the geotechnical design and to assess the effect of such loading on the overall response of the system.

4.2 *Overview of laboratory tests campaign*

In addition to standard index and classification testing, advanced testing to address the cyclic loading and its impact on the axial and lateral design of the foundation piles, were completed. The summary overview and their primary application to design is shown in Table 1.

Given the focus of this paper, monotonic and cyclic DS-CNS tests are further discussed below.

Table 1. Laboratory testing campaign and primary application to design.

Laboratory test description	Primary application
Water content, PSD (Sieve analyses and hydrometer tests), Atterberg limits,	Soil behaviour type classification
Total and dry unit weight	Static design
Particle density, minimum and maximum index unit weight	Reconstitution
pH values	Aggressivity
Carbonate and organic content	Chemical content
IL oedometer tests	Axial design, CPT method
UU test (onshore and offshore – undisturbed)	Static design
UUr test (onshore and offshore – remoulded)	Static design (CPT method)
CIU, CAU, CID and CAD test	Static design
DS-CNS tests, Cyclic DS-CNS tests	CPT based design, axial cyclic degradation, interface strength
DSS test (constant volume), Cyclic DSS test (seismic and Environmental)	Lateral design, seismic design
Resonant column test, bender element test	Seismic site response analysis
Cyclic triaxial test	Lateral design, seismic design

4.3 *Monotonic and cyclic DS-CNS tests*

For evaluating the effect of cyclic loading on the axial soil-pile interaction a series of single-staged, two-way (applied average shear stress/displacement of zero) cyclic direct shear tests with constant normal stiffness (cyDS-CNS) were performed. The majority of these tests were performed as stress-controlled with a constant shear stress applied, whilst a few of these where performed as displacement-controlled with a constant displacement applied for all load cycles throughout the tests. The cyDS-CNS tests were performed as soil-soil tests as well as soil-steel interface tests. For each of the cyDS-CNS tests a monotonic reference test was performed. The peak shear strength of the monotonic reference tests, $\tau_{peak,ref}$, was adopted for the normalization of the applied cyclic shear stress, τ_{cy}, in the cyDS-CNS tests, i.e. the cyclic stress ratio (CSR) was set as given in Eq. 1.

$$CSR = \frac{\tau_{cy}}{\tau_{peak,ref}} \tag{1}$$

The displacement-controlled cyclic tests were performed to evaluate the degradation when the soil is exposed to cyclic loading inducing cyclic displacements (shear strains) larger than or representative of the displacement (shear strain) at peak shear stress in the monotonic tests. Due to the long flexible piles the relative settlement between pile and soil varies significantly along the embedded pile length for a given load level, and therefore also the mobilization of shaft resistance will for a given load level vary significantly along the embedded pile length. Hence, the relevance of performing displacement-controlled cyDS-CNS tests to evaluate the cyclic degradation in the soil present in the shallow part of the pile embedment.

The constant normal stiffness, K, considered for the cyDS-CNS tests was determined based on Eq. 2, as per Johnston et al (1987). considering the shear modulus, G, of the soil material. Conservatively, a shear modulus representative of small-strain was considered. In Eq. 2, D represents the outer pile diameter.

$$K = \frac{4G}{D} \tag{2}$$

It is noted that minor soil loss, ranging between 0.0 to 2.5% of the initial sample weight, was observed for the cyDS-CNS tests. This soil loss is a known issue when performing cyclic direct shear tests and the amount of the soil loss depends on the soil type. For cyDS-CNS tests the soil loss results in a false contractile behaviour and therefore in reduction of normal stresses. The measured normal stresses, σ_n, were corrected, $\sigma_{n,corr}$ through Eq. 3, where W_{loss} represents the weight of the soil loss, W_0 represents the initial sample weight and H_0 represents the initial sample height. As the soil loss was measured at the end of the cyclic tests only, the corrected normal stress could only be evaluated accurately for the final load cycle of the cyDS-CNS tests.

$$\sigma_{n,corr} = \sigma_n + \left(\frac{W_{loss}}{W_0}\right) \cdot H_0 \cdot K \tag{3}$$

The reduction in normal stress with cyclic loading has been evaluated from the cyDS-CNS tests for each of the soil units encountered at the project site. For the stress-controlled cyDS-CNS tests Eq. 4 have been fitted to the test results, where $\Delta\sigma'_r/\sigma'_{r0}$ is the reduction of radial stresses acting on the pile wall due to cyclic axial loading, $\Delta\sigma'_n/\sigma'_{n0}$ represents the reduction of normal stress due to cyclic loading in the cyDS-CNS tests, A, B and C are dimensionless constants, and N is the number of load cycles. Eq. 4 was originally proposed by Jardine et al. (2012).

$$\frac{\Delta\sigma'_r}{\sigma'_{r0}} = \frac{\Delta\sigma'_n}{\sigma'_{n0}} = A\left(B + \frac{\tau_{cy}}{\tau_{peak,ref}}\right) \cdot N^C \tag{4}$$

In Figure 1, the measured reduction of normal stresses for the cyDS-CNS tests performed on a sand soil unit at the Project site is presented with also the fitted relationship, cf. Eq. 4.

Due to the uncertainties related to the performed cyDS-CNS tests caused by the soil loss, the calibration of the dimensionless constants A, B and C was not optimized. It was found that for the sand soil unit of the Project site, use of the values presented in Jardine et al. (2012) valid for Dunkirk sand showed an acceptable match. These values were therefore adopted for the constants A, B and C. It is noted that the test results show a logarithmic dependency between the degradation of the normal stresses and the number of cycles, whilst Eq. 4 adopts an exponential dependency. Hence, an equation with a logarithmic dependency could have offered a better fit to the test results. However, for the number of cycles which are considered of main relevance, the exponential dependent equation, cf. Eq. 4, results in an acceptable fit.

The reduction of normal stress from the displacement-controlled tests has been evaluated and is presented in Figure 2. On Figure 2 a piecewise semi-logarithmic fit to the test results is also presented. It is emphasized that for all displacement-controlled tests a cyclic displacement of 5 mm was adopted.

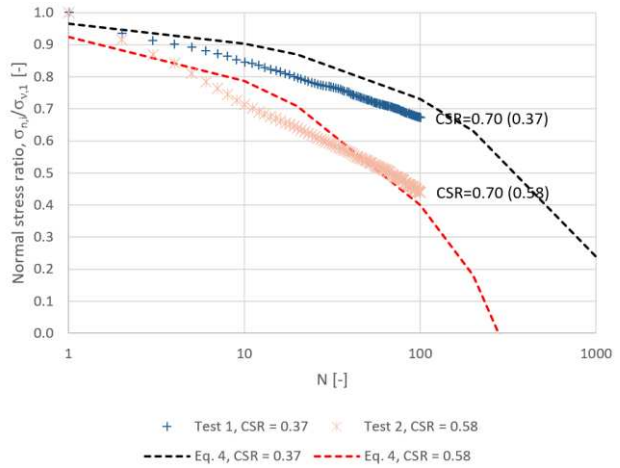

Figure 1. Reduction of normal stress with applied number of load cycles for two stress-controlled cyDS-CNS tests performed on sand soil unit at Project site. The dashed curves represent Eq. 4 with the calibrated values for A=-0.126, B=0.100 and C=0.450.

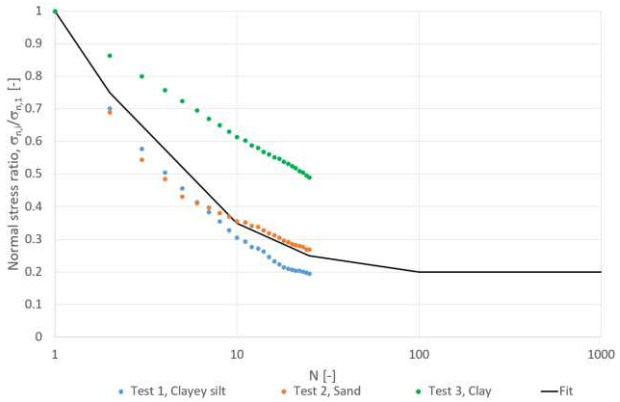

Figure 2. Reduction of normal stress with applied number of load cycles for displacement-controlled cyDS-CNS tests performed on soils at Project site.

In comparison the monotonic DS-CNS tests generally reached peak shear stress at a displacement of approximately 1-2 mm. Hence, the cyclic displacement induced in the displacement-controlled cyDS-CNS tests for each load cycle loads the specimen beyond its peak strength. This may explain the significant amount of degradation measured for these tests, and hence these tests are only representative for scenarios for which the soil is loaded cyclically to displacement levels larger than the displacement at peak shear strength. Limited number of displacement-controlled cyDS-CNS tests were performed. Hence it was not possible to determine a soil unit dependent fit to the test results.

5 DESIGN STORM EVENT

The soil around jacket piles may be exposed to cyclic loading from both environmental loading applied onto the pile and from seismic events. This paper deals only with the cyclic behaviour caused by environmental conditions. Environmental loading acting on the jacket may result in both cyclic lateral loading and cyclic axial loading of the jacket pin-piles. Such cyclic loading may lead to pore-pressure build up, permanent strains, degradation of stiffness and strength of the soil but also of the soil-pile interface. In that regard, this paper addresses the effect of the cyclic loading on the axial pile capacity.

5.1 *Standards*

In accordance with DNVGL (2018), the effects of cyclic loading on the soil-pile interaction shall be evaluated for ULS and SLS conditions. DNVGL (2018) state that cyclic degradation shall be evaluated for the following situations:

- for single storms,
- for normal operating conditions followed by a storm or an emergency shutdown,
- for several succeeding storms,
- and for any other wind and wave load condition that may influence the soil properties.

BSH (2015) suggests that the potential bearing capacity reduction of a foundation which is subject to cyclic loading during a major storm event is analysed considering the complete spectrum. The storm event shall include the design extreme value acting on the foundation elements and the number and distribution of extreme values used must be typical of the particular site. The design event used to verify bearing stability under cyclic loading is described based on the design load case DLC 6.1, cf. DNVGL (2016). BSH (2015) provides recommendations for the variation of wind speed and significant wave height during the ULS storm event. These recommendations are however, developed for the conditions in the German part of the North Sea and Baltic Sea. Hence, a site-specific storm event has instead been established based on the approach of Rezvani et al. (2019) considering recorded storm events, which have occurred within the vicinity of the site.

5.2 *Establishing Markov matrix* representing the cyclic and average loads for the ULS storm event

Wind loads acting on the wind turbines as well as hydrodynamics loads acting on the jacket structure are calculated in the form of time series. Those time series characterise the loads for the recognised stages of the storm, i.e. (i) the build-up of the storm, (ii) the peak of the storm, in which the ultimate design load is embedded, and finally (iii), the decay of the storm.

A load transfer from jacket to pin-piles need be computed with rather sophisticated model of the jacket and pin-piles to fully capture the loading conditions on the pin-piles.

Common engineering practice often describe transient loading through a so-called Markov matrix, which is defined via rainflow counting of the cycles of the storm event and dividing the storm into batches of load cycles for a given cyclic amplitude and average load acting at pile head. The output of such Markov matrix is illustrated in Figure 3.

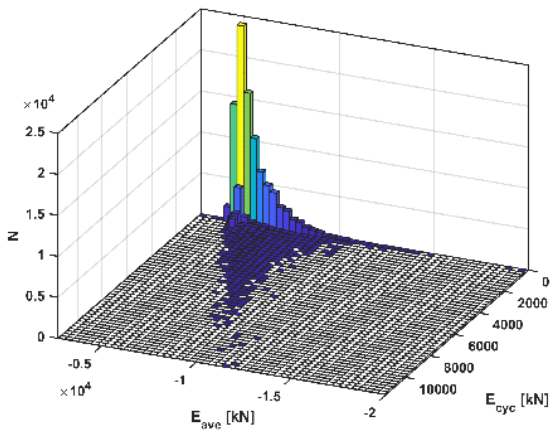

Figure 3. Position-specific Markov matrix for a pile in compression.

6 ESTABLISHED CYCLIC CONCEPT

6.1 *Location-specific cyclic stability diagram*

6.1.1 *Premise*

As mentioned earlier, cyDS-CNS tests can be used to understand the development of radial stress at pile-soil interface with respect to CSR and number of cycles for difference soil deposits, a so-called degradation law. Several authors (e.g. Jardine et al. (2005) or Lehane et al. (2007 and 2013)) have argued that the radial stress around the pile is closely related to the shaft capacity R_{sk}. By extension to Eq. 4, the decrease in shaft resistance ΔR_{sk} can be related to the number of cycles N, and to the cyclic amplitude at pile head, E_{cyc}, see Eq. 5.

$$\frac{\Delta R_{sk}}{R_{sk}} = A\left(B + \frac{E_{cyc}}{R_{sk}}\right) \cdot N^C \qquad (5)$$

Furthermore, based on the Winkler model and *t-z* curves mentioned earlier, one may go further so that the degradation law in Eq. 4 and Eq. 5 can be modified to Eq. 6 for a given depth along the pile, where t_{mob}/t_{max} is analogous of the utilisation of the *t-z* curve.

$$\frac{\Delta t}{t_{max}} = A\left(B + \frac{t_{mob}}{t_{max}}\right) \cdot N^C \qquad (6)$$

The constants of this equation are derived from the stress-controlled DS-CNS tests and are seen as representative of small-strain behaviour. Contrarily, displacement-controlled tests show relatively large displacements and a much steeper loss of normal stress with respect to number of cycles, which may then be used to model large-displacement degradation.

The fits to the stress- and displacement-controlled DS-CNS tests discussed in section 4.3 are referred further as degradation laws.

6.1.2 *Algorithm*

The algorithm used to determine the cyclic interaction diagram is based upon the use of a 1D beam Winkler model with t-z curves. The different steps are listed below and illustrated in Figure 4.

- Step 1 – Several static displacement-controlled analyses are performed for the relevant soil profile and tentative pile geometry in a 1D Winkler model with *t-z* curves. The displacement at pile head is noted as u_z while z_{peak} is a feature of the t-z curves that is considered as 1% of the pile outer diameter (API, 2014).
- Step 2 – Shaft resistance and mobilised t-z curves are extracted and saved. This step also ensures that the mobilised capacity of the pile match the analytical method.
- Step 3 – The 1D Winkler model are run for N > 1, in a static-manner, but with the inclusion of cyclic degradation as per degradation laws. The small-displacement degradation law is used for $t_{mob}/t_{max} < 1$ and vice-versa, ensuring a larger degradation for the upper part of the pile, as expected from a theoretical standpoint.
  - Step 3a – This step starts the iterative process which aims to find a converging ratio t_{mob}/t_{max}. The first iteration starts assuming $\Delta t = 0$ along the entire pile, i.e. no cyclic degradation on the *t-z* curves. Δt represents the degradation of shaft resistance.
  - Step 3b – Δt is extracted once convergence is ensured and pile head displacement u_z is increased.
- Step 4 – The shaft mobilisation calculated for a given number of cycles and with a converged t_{mob}/t_{max} is plotted against the applied pile head displacement.
- Step 5 – The maximum shaft mobilisation $R_{sk,mob}$ is extracted and used as basis to define the contours on the ordinate axis.
- Step 6 – The contour diagram is finalised by the following assumption: all contours are made to converge at the point $\left(\frac{E_{ave}}{R_{sk}} = 1, \frac{E_{cyc}}{R_{sk}} = 0\right)$. This assumption merely suggests that this point on the cyclic interaction diagram relates to a static loading condition, as no cyclic component would occur, and where the mean contribution of cyclic loading, E_{ave}, matches the shaft capacity.

One of the advantages of the above approach is that it takes into account the axial flexibility of the pile, and hence that the mobilisation of the shaft resistance will vary with depth and hence also that the degradation of the shaft resistance will vary with depth.

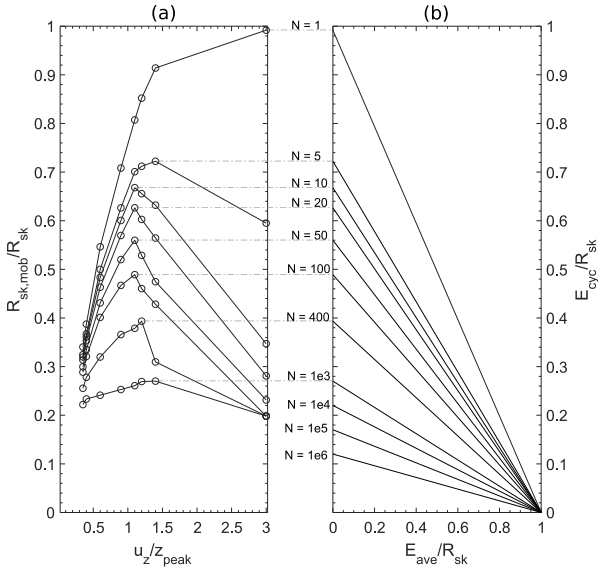

Figure 4. (a) Displacement-controlled 1-D model (Winkler foundation with t-z curves) with mobilised shaft resistance along the pile. (b) Resulting cyclic interaction diagram.

6.2 *Degraded shaft resistance*

The degradation model established in this section is based upon the work of Stuyts et al. (2012). This approach uses the cyclic contour diagram to determine the number of cycles to failure for a given entry of the markov matrix, i.e. a couple (E_{ave}, E_{cyc}). A loop to all Markov matrix entries is performed, and a degradation factor is calculated for use in the analytical axial pile capacity method. Further details are captured in Figure 5.

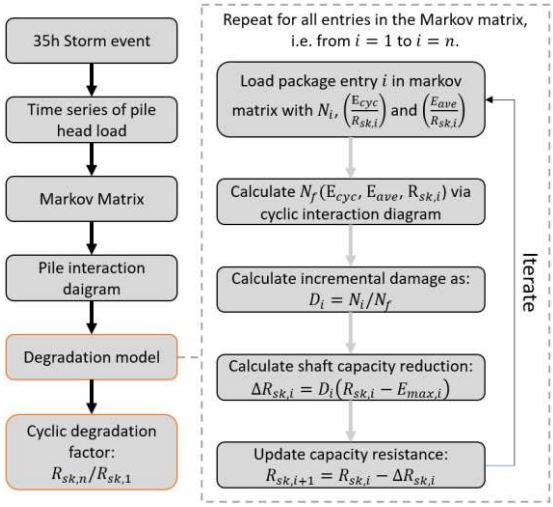

Figure 5. Degradation model used to reduce shaft resistance.

Figure 6 shows all the entries of the Markov matrix plotted on the cyclic contour diagram for the governing tension and compression pile of a jacket foundation. For each bin, a damage

contribution may be calculated. This damage law is assumed linear, cf. Eq. 7, and assumes that for full damage, $D_i = 1$, the degraded shaft resistance must be equal to the considered load level, $E_{max} = E_{cyc} \pm E_{ave}$, as failure would occur.

$$D_i = \frac{N_i}{N_f} \tag{7}$$

The cyclic degradation factor for the final pile geometries across the site ranged from 92% to 99%, i.e. a loss of shaft capacity of up to 8%.

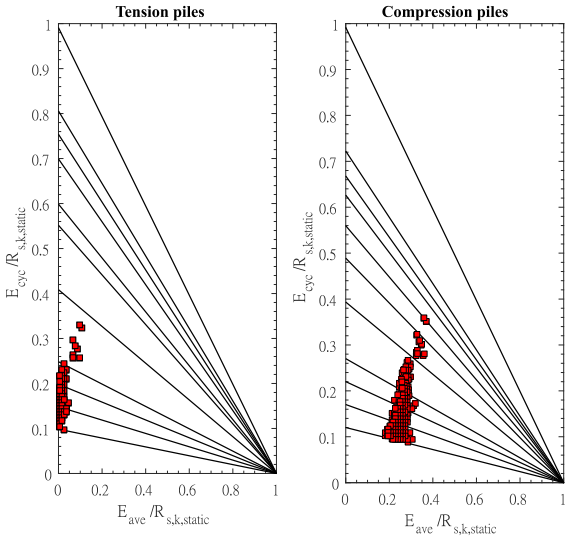

Figure 6. Design storm event plotted on cyclic pile interaction diagrams for most onerous tension and compression piles. Each dot represents one bin of the Markov matrix.

7 CONCLUSION

This paper presents the methodology used for the cyclic concept of jacket pin-piles supporting wind turbines at a site in the Taiwanese strait. The paper focuses on the axial pile capacity, design driver of such foundation piles.

The lack of documentation in design codes and standards led to the use of an approach to derive cyclic interaction diagram via the commonly used Winkler model (a 1D beam model supported by independent springs along the axis of the pile) and the observed cyclic soil behaviour from advanced laboratory testing.

Site-specific conditions were incorporated in this diagram as an advanced laboratory campaign with static and cyclic DS-CNS tests permitted the extraction of normal stress with respect to the number of cycles to estimate the loss of radial stress along the pile.

A degradation model, based on the work presented by Stuyts et al (2012) was considered to degrade the shaft resistance of the pile, and a Markov matrix ensured the site-specific loading conditions were considered. Results of this study showed a cyclic degradation of up to 8% of the shaft resistance available for static loading conditions.

The method presented here gathers results from laboratory testing and state-of-the-art design methodology to establish a practical framework for designers to estimate the cyclic degradation of axial pile design. Further works could include the benchmark of this method against *in-situ* pile tests with further calibration of the degradation laws.

8 REFERENCES

API (2014): API 2A-WSD. Recommended Practice for Planning, Designing and Constructing Fixed Offshore Platforms – WorkingStress Design. 22nd Edition. November 2014.

Argiolas, R. and Jardine, R. (2017): An integrated pile foundation reassessment to support life extension and new build activities for a mature North Sea oil field project. In Proceedings of Offshore Site Investigation and Geotechnics, London, UK.

BSH (2015): Standard Design – Minimum requirements concerning the constructive design of offshore structures within the Exclusive Economic Zone (EEZ). Bundesamt für Seeschifffahrt und Hydrographie.

Clausen, C. F. J., Aas, P. M. and Karlsrud, K. (2005): Bearing capacity of driven piles in sand, the NGI approach. In Proceedings of Frontiers in Offshore Geotechnics, ISFOG, pp. 677-681.

DNVGL (2016): DNVGL-ST-0437, Loads and site conditions for wind turbines, edition November 2016.

DNVGL (2018): DNVGL-ST-0126, Support structures for wind turbines. Edition July 2018.

Dührkop, J. (2010): Zum Einfluss von Aufweitungen und Zyklischen Lasten auf das Vermungsverhalten Lateral beanspruchter Pfähle in Sand. In TU Hamburg, Veröffentlichungen des Instituts für Geotechnik und Baubetrieb, Heft 20.

Gavin, K., Igoe, D. and Doherty, P. (2011). Piles for offshore wind turbines: a state-of-the-art review. Geotechnical Engineering, 164(4), pp. 245-256.

GWEC (2021): Global Offshore Wind Report 2021. https://gwec.net/global-offshore-wind-report-2021/

Hampson, K., Evans, T. G., Jardine, R. J., Moran, P., Mackenzie, B. and Rattley, M. J. (2017): BP Clair Ridge: Independent foundation assurance for the capacity of driven piles in very hard soils. In Proceedings of Offshore Site Investigation and Geotechnics, London, UK.

Jardine, R.J., Chow, F.C., Overy, R. and Standing, J.R. (2005). ICP Design Methods for Driven Piles in Sands and Clays. Thomas Telford Publishing.

Jardine, R., Puech, A. and Andersen, K. H. (2012): Cyclic loading of offshore piles: Potential effects and practical design. In Proceedings of Offshore Site Investigation and Geotechnics: Integrated Technologies – Present and Future, London, UK.

Johnston I. W., Lam, T. S. K., and Williams, A. F. (1987): Constant Normal Stiffness Direct Shear Testing for Socketed Pile Design in Weak Rock. Geotechnique, No. 37, pp 83-89.

Karlsrud, K., Clausen, C. J. F. and Aas, P. A. (2005): Bearing capacity of driven piles in clay, the NGI approach. In Proceedings of Frontiers in Offsore Geotechnics, ISFOG, pp. 775-782.

Kirsch, F., and Richter, T. (2011). Ein einfaches Näherungsverfahren zur Prognose des axialzyklischen Tragverhaltens von Pfählen, Bautechnik 88, Heft 2, 113–120.

Lehane, B., Schneider, J., and Xu, X. (2007). Development of the UWA-05 design method for open and closed ended driven piles in siliceous sand. In H. W. Olsen (Ed.), Proceedings of Geo-Denver 2007 (Denver, USA ed., Vol. GSP 157-174, pp. online). American Society of Civil Engineers.

Lehane, B., Li, Y., and Williams, R. (2013). Shaft Capacity of Displacement Piles in Clay Using the Cone Penetration Test. Journal of Geotechnical and Geoenvironmentral Engineering, 139, 253-266.

Merritt, A. S., Schroeder, F.C., Jardine, R. J., Cathie, D. and Cleverly, W. (2012): Development of pile design methodology for an offshore wind farm in the North Sea. In Proceedings of Offshore Site Investigation and Geotechnics, London, UK.

Poulos H. G. (1989): Pile behaviour – Theory and Application. In Géotechnique 39, No. 3, 365-415.

Stuyts, B., Cathie, D., Falepin, H. and Burgraeve, A. (2012): Axial pile capacity of wind turbine foundations subjected to cyclic loading. In Proceedings of Offshore Site Investigation and Geotechnics: Integrated Technologies – Present and Future, London, UK.

Rezvani, S., Bundesen, J., Skourup, J. and Melin, G. (2019) An optimized approach in geotechnical design using locally prescribed storm event. In Proceedings of 16th Asian Regional Conference, Taipei, Taiwan.

Winkler, E., 1867. Die Lehre von der Elasticitaet und Festigkeit. Prague: Dominicus, (in German)